JCI The Journal of Clinical Investigation

TSC1 regulates the balance between effector and regulatory T cells

Yoon Park, … , Mitchell Kronenberg, Yun-Cai Liu

J Clin Invest. 2013;123(12):5165-5178. https://doi.org/10.1172/JCI69751.

Research Article

Mammalian target of rapamycin (mTOR) plays a crucial role in the control of T cell fate determination; however, the precise regulatory mechanism of the mTOR pathway is not fully understood. We found that T cell–specific deletion of the gene encoding tuberous sclerosis 1 (TSC1), an upstream negative regulator of mTOR, resulted in augmented Th1 and Th17 differentiation and led to severe intestinal inflammation in a colitis model. Conditional *Tsc1* deletion in Tregs impaired their suppressive activity and expression of the Treg marker Foxp3 and resulted in increased IL-17 production under inflammatory conditions. A fate-mapping study revealed that *Tsc1*-null Tregs that lost Foxp3 expression gained a stronger effector-like phenotype compared with $Tsc1^{-/-}$ $Foxp3^{+}$ Tregs. Elevated IL-17 production in $Tsc1^{-/-}$ Treg cells was reversed by in vivo knockdown of the mTOR target S6K1. Moreover, IL-17 production was enhanced by Treg-specific double deletion of *Tsc1* and *Foxo3a*. Collectively, these studies suggest that TSC1 acts as an important checkpoint for maintaining immune homeostasis by regulating cell fate determination.

Find the latest version:

https://jci.me/69751/pdf

TSC1 regulates the balance between effector and regulatory T cells

Yoon Park,[1] Hyung-Seung Jin,[1] Justine Lopez,[1] Chris Elly,[1] Gisen Kim,[2] Masako Murai,[2] Mitchell Kronenberg,[2] and Yun-Cai Liu[1]

[1]Division of Cell Biology, and [2]Division of Developmental Immunology, La Jolla Institute for Allergy and Immunology, La Jolla, California, USA.

Mammalian target of rapamycin (mTOR) plays a crucial role in the control of T cell fate determination; however, the precise regulatory mechanism of the mTOR pathway is not fully understood. We found that T cell–specific deletion of the gene encoding tuberous sclerosis 1 (TSC1), an upstream negative regulator of mTOR, resulted in augmented Th1 and Th17 differentiation and led to severe intestinal inflammation in a colitis model. Conditional *Tsc1* deletion in Tregs impaired their suppressive activity and expression of the Treg marker Foxp3 and resulted in increased IL-17 production under inflammatory conditions. A fate-mapping study revealed that *Tsc1*-null Tregs that lost Foxp3 expression gained a stronger effector-like phenotype compared with *Tsc1*$^{-/-}$ Foxp3^{+} Tregs. Elevated IL-17 production in *Tsc1*$^{-/-}$ Treg cells was reversed by in vivo knockdown of the mTOR target S6K1. Moreover, IL-17 production was enhanced by Treg-specific double deletion of *Tsc1* and *Foxo3a*. Collectively, these studies suggest that TSC1 acts as an important checkpoint for maintaining immune homeostasis by regulating cell fate determination.

Introduction

Mammalian target of rapamycin (mTOR), a conserved Ser/Thr protein kinase, functions as a sensor of the cellular nutrient and energy status and regulates metabolism, protein synthesis, and proliferation (1, 2). It exists in two forms, either mTOR complex 1 (mTORC1) or complex 2 (mTORC2), which are characterized by their assembly with different signaling proteins (3). Recent studies have revealed that the mTOR signaling pathway is crucially involved in the process of T cell fate determination, including the differentiation of naive cells into either effector or regulatory T (Treg) cells and the development of CD8 memory T cells (4–8). Genetic ablation of mTOR in mice results in the failed differentiation of T helper (Th) 1, 2, and 17 cells, whereas mTOR-deficient T cells become Foxp3^{+} Treg cells when activated (9). The important role of mTOR in regulating Foxp3^{+} Treg cell responsiveness or stability has been implicated by studies of the mTOR inhibitor rapamycin (10, 11). More recent studies of Rheb- or Rictor-deficient mice suggest that distinct mTORC1 or mTORC2 activities selectively regulate each subset of effector T cells, but inhibition of both activities is required for the spontaneous generation of Foxp3^{+} Treg cells (6). Despite all these findings, regulation of the mTOR pathways in Th/Treg differentiation and the underlying immune responses are still not fully understood.

Tuberous sclerosis complex 1 (TSC1 or hamartin), which forms a heterodimeric complex with TSC2 (tuberin), inhibits mTORC1 by promoting the conversion of guanosine triphosphate (GTP) into guanosine diphosphate (GDP) on the mTORC1 activator Rheb. Genetic deletion of TSC1 or TSC2 causes constitutive activation of mTORC1 signaling, leading to the attenuation of PI3K signaling (12). The important function of TSC1 in T cell activation and homeostasis was recently demonstrated by an analysis of mice with TSC1-deleted T cells (13–17); hyperactivation of mTORC1 in these TSC1-deficient T cells resulted in a survival defect, loss of quiescence, and resistance to T cell anergy, which disrupted T cell homeostasis. However, the influence of TSC1 on the interplay between Th and Treg cell responses, particularly under inflammatory conditions, still remains unknown.

Several studies have suggested that Treg cells exhibit phenotypic and functional plasticity that allows them to reprogram into effector-type T cells that can adapt to microenvironmental changes (18–21). To trace the fates of Foxp3^{+} Treg cells in vivo, Zhou et al. generated double-transgenic reporter mice to demonstrate that Treg cells can lose Foxp3 expression to become Foxp3-negative "ex-Treg" cells and acquire an effector or memory cell phenotype under autoimmune conditions (22). However, another study provided evidence that Treg cells are stable under various inflammatory conditions (23). It was more recently suggested that the committed Treg cells sustain Foxp3 expression and refrain from reprogramming, whereas only uncommitted Treg cells could convert into "ex-Treg" cells (24). Obviously, the regulatory mechanism for determining the stability and maintenance of Treg cells remains to be addressed.

To address these issues, we generated mice with a conditional deletion of TSC1 in either T cells or Treg cells, together with a fate-mapping approach, and we studied the role of TSC1 in modulating Th17 and Treg cell responses under normal and inflammatory conditions. Our results suggest an essential role of TSC1 in modulating Th cell differentiation and Treg cell conversion and stability in response to environmental cues via the regulation of both mTORC1 and mTORC2 signaling pathways.

Results

TSC1 is required to maintain mucosal immune homeostasis. In order to more precisely understand how the mTOR pathway is involved in the regulation of CD4^{+} T cell responses, we bred mice carrying a loxP-flanked *Tsc1* allele with mice expressing Cre recombinase from the CD4 promoter to delete TSC1 specifically in T lymphocytes (referred to herein as *Cd4*^{Cre}*Tsc1*$^{f/f}$ mice). Since it has been reported that TSC1 deficiency in T cells results in enhanced T cell activation (15, 17), we monitored WT and *Cd4*^{Cre}*Tsc1*$^{f/f}$ mice over

Conflict of interest: The authors have declared that no conflict of interest exists.
Citation for this article: *J Clin Invest.* 2013;123(12):5165–5178. doi:10.1172/JCI69751.

20 weeks of age for clinical signs of autoimmunity. Histological staining of colon and liver sections revealed that *Cd4^{Cre}Tsc1$^{f/f}$* mice, but not WT mice, spontaneously developed inflammation characterized by lymphocyte infiltration and large lymphoid aggregates (Figure 1A).

Because effector T cells of the adaptive immune system may play a role in sustaining rather than initiating intestinal inflammation, which in many cases is driven by the innate immune system (25), we used a dextran sodium sulfate–induced (DSS-induced) model of chronic colitis to assess the progression from the acute to the chronic phase in *Cd4^{Cre}Tsc1$^{f/f}$* mice. We exposed the WT and *Cd4^{Cre}Tsc1$^{f/f}$* mice to 2% DSS in the drinking water for 7 days and analyzed them up to 4 weeks after DSS removal (Figure 1B). We recorded body weight loss during the DSS treatment and recovery period. *Cd4^{Cre}Tsc1$^{f/f}$* mice showed a relatively rapid and more severe weight loss. Also, the recovery from weight loss in *Cd4^{Cre}Tsc1$^{f/f}$* mice was much slower after DSS removal compared with that in WT mice (Figure 1C). On day 28, we observed colon length shortening (Figure 1D) and a substantial increase in the size of the spleen and mesenteric lymph nodes (MLNs) (Figure 1E) in *Cd4^{Cre}Tsc1$^{f/f}$* mice compared with that found in WT mice. *Cd4^{Cre}Tsc1$^{f/f}$* mice also displayed more severe lymphocytic infiltration and destruction of epithelial architecture in the colon on day 28 (Figure 1F) and even up to day 35 (Supplemental Figure 1A; supplemental material available online with this article; doi:10.1172/JCI69751DS1). Collectively, these results suggest that TSC1 deficiency in CD4$^+$ effector T cells leads to an increased susceptibility to intestinal inflammation.

We next examined the production of proinflammatory cytokines by CD4$^+$ T cells in the colon and spleen of DSS-treated mice. On day 28, there was a significant increase in IFN-γ and IL-17A production by TSC1-deficient CD4$^+$ T cells (Figure 1G), and this increase was sustained until day 35 (Supplemental Figure 1B). There was no appreciable difference, however, between WT and *Cd4^{Cre}Tsc1$^{f/f}$* mice under both basal and acute colitis conditions with 3% DSS (Supplemental Figure 2). Taken together, we demonstrate a crucial role for TSC1 in restricting a proinflammatory T cell response that prevented the development of chronic intestinal inflammation and maintained intestinal homeostasis.

TSC1 restricts Th1 and Th17 cell differentiation. We cultured WT and TSC1-deficient naive CD4$^+$ T cells under polarizing conditions for Th1 or Th17 cell differentiation, including coincubation with appropriate cytokines and anticytokine antibodies for 5 days, followed by restimulation with anti-CD3 and anti-CD28. Intracellular cytokine staining for IFN-γ and IL-4 or IL-17A showed that cytokine production from the Th1 and Th17 subsets was substantially increased under polarizing conditions in TSC1-deficient T cells (Figure 2A). This increase was further confirmed by measuring cytokine secretion by ELISA, with concentrations of signature cytokines for Th1 and Th17 responses being markedly increased in the culture supernatants of TSC1-deficient T cells (Figure 2B). Consistently, TSC1-deficient T cells exhibited significantly elevated mRNA levels of *Tbx21* and *Rorc* under Th1- and Th17-polarizing conditions, respectively (Figure 2C). These results indicate that TSC1 is required for the limitation of Th cell differentiation in vitro.

To investigate the biological relevance of TSC1 in Th cell responses, we examined the effect of TSC1 deficiency on the generation of Th1 and Th17 subsets using in vivo mouse models. We adoptively transferred CD4$^+$ T cells from WT or *Cd4^{Cre}Tsc1$^{f/f}$* OVA-specific OT-II transgenic mice into CD45.1 congenic C57BL/6 mice and then immunized them with an OVA peptide plus CFA as an adjuvant. We found that OVA-induced IFN-γ–producing Th1 cells were greatly increased in the mice receiving TSC1-deficient OT-II T cells (Figure 2D, upper panel). Likewise, TSC1 deficiency resulted in an increased IL-17–producing T cell population (Figure 2D, lower panel).

A previous study showed that TSC1-deficient T cells have a survival defect that leads to the loss of adoptively transferred cells in recipient mice (15). To rule out the viability issue of the transferred TSC1-deficient T cells in recipient mice, we immunized WT and *Cd4^{Cre}Tsc1$^{f/f}$* mice with keyhole limpet hemocyanin (KLH) emulsified in CFA. CD4$^+$ T cells from the immunized mice were restimulated in vitro with KLH for 72 hours and examined the supernatants with a Bio-Plex multicytokine assay. Consistent with the adoptive transfer data, we observed an augmented induction of both Th1 and Th17 signature cytokine levels as well as IL-6 in TSC1-deficient CD4$^+$ T cells (Figure 2E), suggesting that TSC1 is an important negative regulator in the generation of Th1 and Th17 cells.

TSC1 deficiency affects the ability of Treg cells to suppress colitis. The increased spontaneous inflammation likely reflected increased effector cell generation, although decreased Treg activity also could have contributed. We therefore examined the effect of TSC1 deficiency on Foxp3 expression induced by TGF-β in cultures that generate adaptive or inducible Treg (iTreg) cells. Sorted CD4$^+$CD62L$^+$CD25$^-$ naive T cells were cultured with anti-CD3 plus anti-CD28 and TGF-β for 4 days and then analyzed by intracellular staining for Foxp3. The induction of Foxp3 expression by TGF-β was similar between WT and TSC1-deficient naive CD4$^+$ T cells (Figure 3A). In a coculture assay to measure suppressive activity, we found that iTreg cells from either WT or *Cd4^{Cre}Tsc1$^{f/f}$* mice effectively inhibited naive CD4$^+$ T cell division (Figure 3B), which indicated that TSC1 is not required for the in vitro differentiation and suppressive function of iTreg cells triggered by TGF-β.

Although the generation and function of TSC1-deficient iTreg cells were intact in vitro, we reasoned that the breakdown of intestinal immune homeostasis in *Cd4^{Cre}Tsc1$^{f/f}$* mice may be caused not only by increased production of proinflammatory effector cytokines, but also by impaired Treg cell homeostasis or function under inflammatory conditions. Indeed, *Cd4^{Cre}Tsc1$^{f/f}$* mice with chronic DSS-induced colitis (day 28) displayed a decrease in the percentage of Foxp3$^+$ Treg cells in the spleen compared with that observed in WT mice, and this difference was even more pronounced in colonic lamina propria (cLP) (Supplemental Figure 3). To further investigate whether TSC1 deficiency in Treg cells is associated with the development of colitis, we cotransferred sorted CD4$^+$CD45RB^{hi} (CD45.1$^+$) naive T cells with or without sorted CD4$^+$CD45RB^{lo}CD25$^+$ (CD45.2$^+$) Treg cells from either WT or *Cd4^{Cre}Tsc1$^{f/f}$* mice into *Rag1$^{-/-}$* mice and recorded their body weight changes for over a 12-week period. *Rag1$^{-/-}$* mice that received TSC1-deficient Treg cells gained weight until 6 weeks after transfer, but then started to lose weight and finally lost around 10% of their body weight at 12 weeks (Figure 3C). Consistent with the weight loss, the recipient mice that were either transferred with CD4$^+$CD45RB^{hi} T cells alone or cotransferred with TSC1-deficient CD4$^+$CD45RB^{lo}CD25$^+$ Treg cells developed inflammation with enlargement of the spleen and MLNs (data not shown) and colitis with histological features of intestinal disease (Figure 3D). By contrast, the recipient mice that were given WT CD4$^+$CD45RB^{lo}CD25$^+$ Treg cells were resistant to the develop-

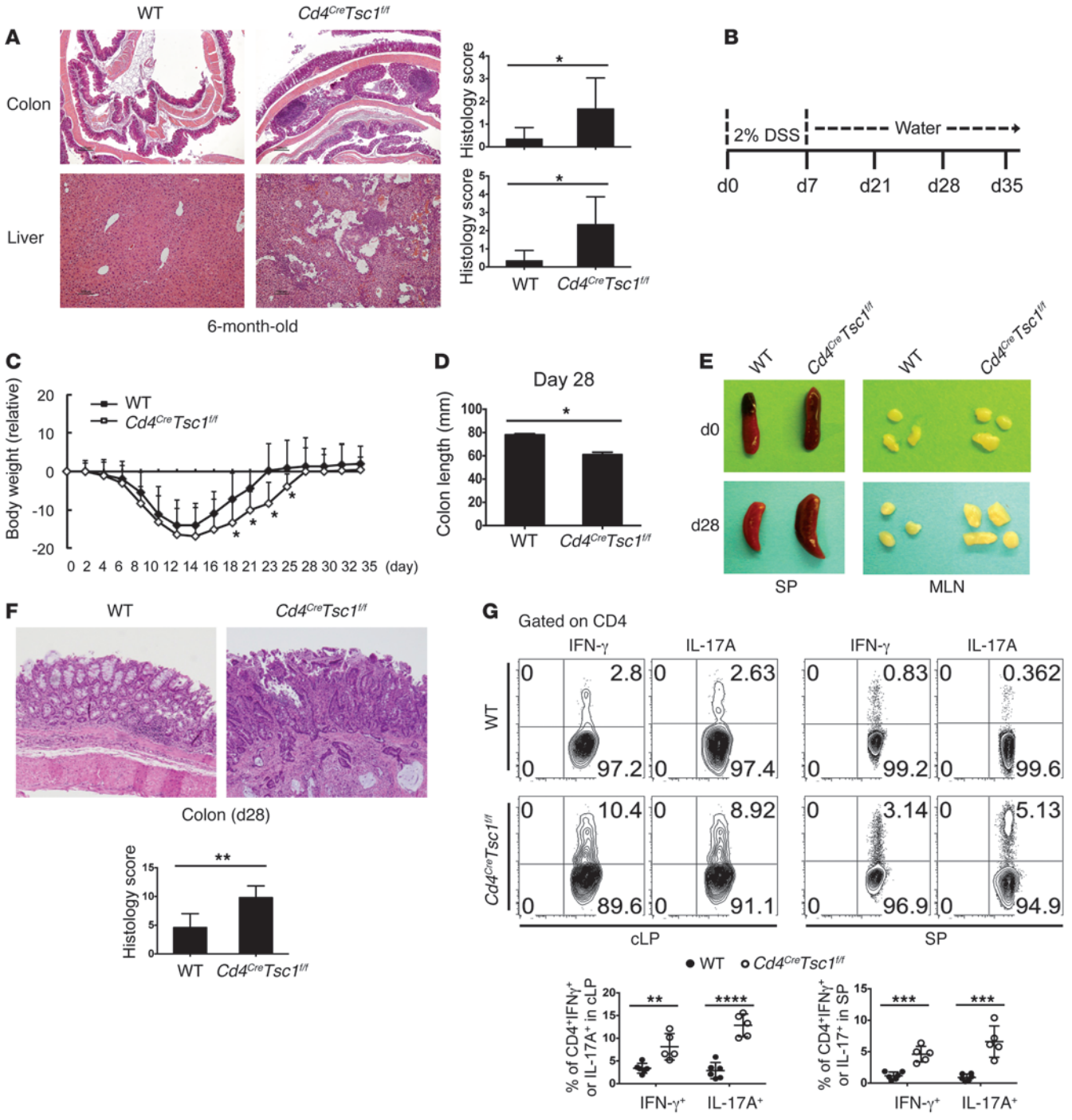

Figure 1

TSC1 function in T cells preserves intestinal homeostasis. (**A**) H&E staining and histological scores of colon and liver tissue sections from 6-month-old mice. Original magnification, ×100. Data are representative of (left) and compiled from (right) 6 mice. Error bars indicate the mean ± SD. *$P < 0.05$ by two-tailed, unpaired Student's *t* test. (**B**) Overview of DSS-induced chronic colitis model. Mice were administrated 2% DSS for 7 days followed by water and were analyzed up to 4 weeks later. (**C**) Body weight changes in WT and *Cd4*^{Cre}*Tsc1*$^{f/f}$ mice after DSS treatment. Weight loss of individual mice was monitored every 2 days. Data are compiled from three independent experiments with three mice each. Error bars indicate the mean ± SD. *$P < 0.05$ by two-tailed, unpaired Student's *t* test. (**D**–**F**) Colon length (**D**); photograph of representative spleen (SP) and mesenteric lymph nodes (MLNs) (**E**); H&E staining and histology scores of colon (**F**). Original magnification, ×100 (**F**). (**G**) Flow cytometric analysis of cytokine production (left) and frequencies (right) in colonic lamina propria (cLP) and splenic (SP) CD4$^+$ T cells. Cells were obtained from WT and *Cd4*^{Cre}*Tsc1*$^{f/f}$ mice 3 weeks after DSS removal (day 28) and restimulated in vitro. Data are compiled from (**D**) or representative of (**E**–**G**) three independent experiments. Each symbol represents an individual mouse ($n = 5–6$). Error bars indicate the mean ± SD. *$P < 0.05$, **$P < 0.01$, ***$P < 0.001$, and ****$P < 0.0001$ by two-tailed, unpaired Student's *t* test.

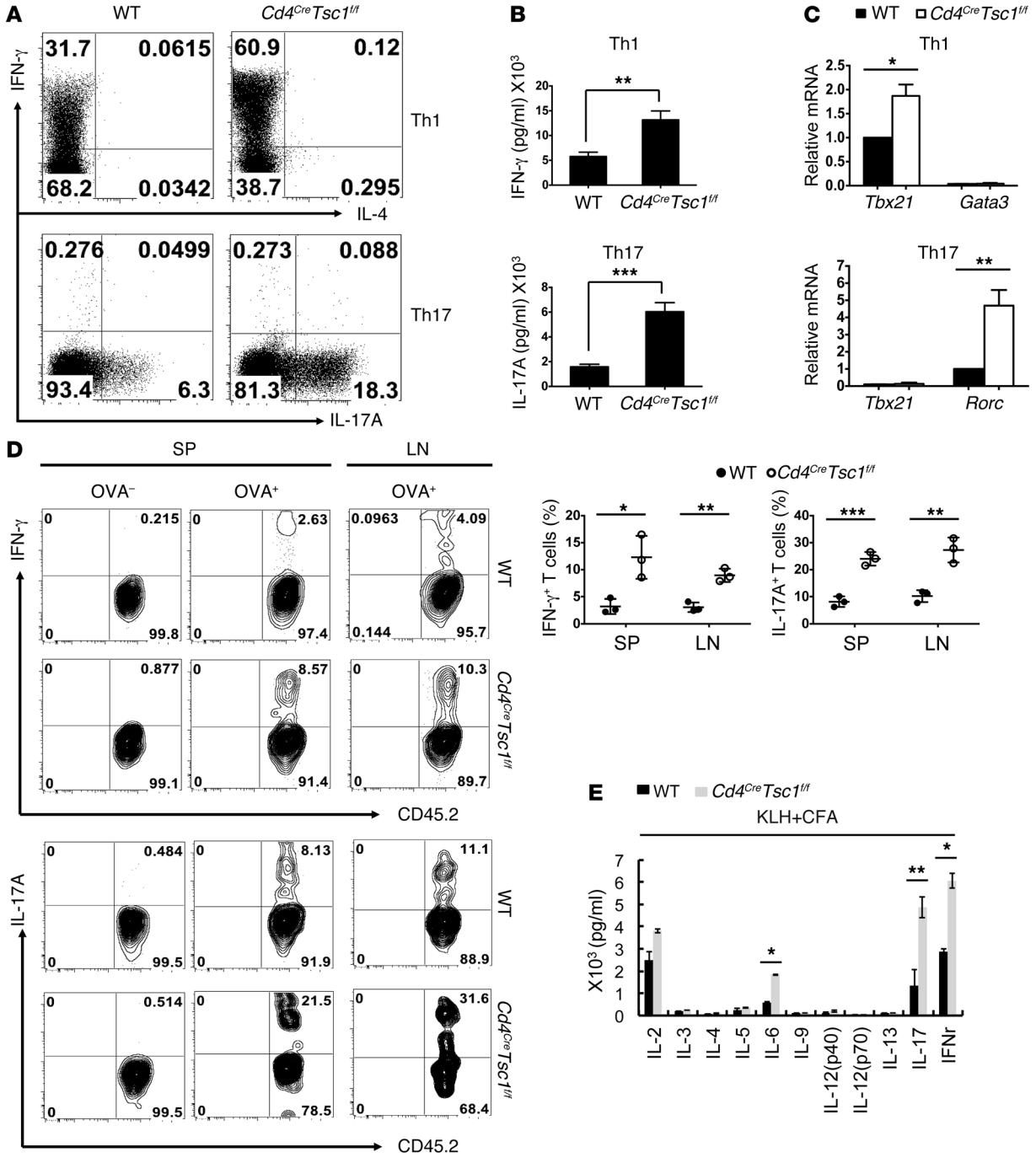

Figure 2

TSC1 deficiency promotes Th1 and Th17 differentiation. (**A**) Naive CD4+ T cells from WT and *Cd4*^{Cre}*Tsc1*$^{f/f}$ mice were cultured under Th1- and Th17-polarizing condition for 5 days. IFN-γ–, IL-4–, or IL-17A–producing cells were analyzed by intracellular cytokine staining (ICCS) 6 hours after restimulation with anti-CD3/CD28. (**B**) Th1 and Th17 cell cytokine production was measured by ELISA 24 hours after restimulation with anti-CD3/CD28. (**C**) RT-PCR analysis of mRNA expression levels of Th subset–specific transcription factors in polarized Th1 or Th17 cells. Data are representative of (**A**) or compiled from (**B** and **C**) three to five independent experiments. Error bars indicate the mean ± SD. **P* < 0.05, ***P* < 0.01, and ****P* < 0.001 by two-tailed, unpaired Student's *t* test . (**D**) IFN-γ and IL-17 production (upper panel) and frequencies (lower panel) in T cells from recipient mice immunized with OVA/CFA. CD4+ T cells from WT or *Cd4*^{Cre}*Tsc1*$^{f/f}$ OT-II mice were adoptively transferred into CD45.1 congenic B6 mice, followed by immunization with OVA/CFA. Splenocytes and lymph node cells obtained 6 days later were stimulated with $OVA_{323–339}$ peptide for 24 hours and analyzed by ICCS and flow cytometry. (**E**) Immunization of WT and *Cd4*^{cre}*Tsc1*$^{f/f}$ mice with KLH/CFA. CD4+T cells obtained 6 days later were stimulated with KLH for 72 hours, and the culture supernatants were analyzed by Bio-Plex multicytokine assay. Data are representative of (**D**) or compiled from (**E**) three independent experiments. Each symbol represents an individual mouse (*n* = 3). Error bars indicate the mean ± SD. **P* < 0.05, ***P* < 0.01, and ****P* < 0.001 by two-tailed, unpaired Student's *t* test.

ment of colitis. These results imply that TSC1 expression by Treg cells is required for the suppression of T cell–induced colitis.

We next analyzed the suppressive activity of transferred Treg cells by analyzing the in vivo expansion of $CD4^+CD45RB^{hi}$ T cells and Treg cells in *Rag1*$^{-/-}$ recipient mice 12 weeks after transfer. In all organs analyzed, the ratio of $CD4^+CD45RB^{hi}$ T cells ($CD45.1^+$)/$CD4^+CD45RB^{lo}CD25^+$Treg ($CD45.2^+$) cells was increased in the recipient mice given TSC1-deficient Treg cells compared with those that received WT Treg cells (Figure 3E). Despite the increased ratio of naive T cells/Treg cells, the total numbers of TSC1-deficient Treg cells were similar to WT Treg cell numbers in most organs analyzed except in colon (Figure 3F), which suggests that the defect in colitis suppression by the transfer of TSC1-deficient Treg cells is not simply a quantitative one related to the increased ratio of effectors/Tregs, but could also be a consequence of the attenuated suppressive activity of TSC1-deficient Treg cells. Indeed, while over 97% of FACS-sorted $CD4^+CD45RB^{lo}CD25^+$ Treg cells were Foxp3 positive before the adoptive transfer (Figure 3G), we found the population that lost Foxp3 expression in the recipient mice given TSC1-deficient Treg cells 12 weeks after transfer (Figure 3H), which suggests a possible role of TSC1 in Treg cell regulation.

Treg-specific TSC1 deletion leads to impaired function under inflammatory conditions. To more precisely assess the intrinsic role of TSC1 in the function of $Foxp3^+$ Treg cells, we bred *Tsc1*$^{f/f}$ mice with *Foxp3*^{Cre} mice expressing a yellow fluorescent protein–Cre (YFP-Cre) recombinase fusion protein under the control of the Foxp3 promoter in order to delete TSC1 specifically in $Foxp3^+$ Treg cells (referred to herein as *Foxp3*^{YFPCre}*Tsc1*$^{f/f}$). TSC1 deficiency in Treg cells had no effect on the development of CD4 or CD8 single- or CD4/CD8 double-positive T cells in the thymus (Supplemental Figure 4A). Despite slightly lower frequencies of $CD4^+$ or $CD8^+$ T cells in peripheral lymphoid tissues such as those found in the spleen of *Foxp3*^{YFPCre}*Tsc1*$^{f/f}$ mice (Supplemental Figure 4, B and C), the absolute numbers of T cells were instead slightly increased, which reflects the expanded population of non–T cells (Supplemental Figure 4D). More importantly, the frequencies of naive ($CD44^{lo}CD62L^{hi}$) and effector/memory ($CD44^{hi}CD62L^{lo}$) $CD4^+$ T cells were similar in *Foxp3*^{YFPCre}*Tsc1*$^{+/+}$ and *Foxp3*^{YFPCre}*Tsc1*$^{f/f}$ mice (Supplemental Figure 4, E and F). These data imply that TSC1 deficiency in Treg cells did not affect T cell differentiation or homeostasis.

We then examined the effect of TSC1 deficiency on Treg cell homeostasis. $CD4^+YFP^+$ Treg cell frequencies were decreased in both the spleen and cLP of *Foxp3*^{YFPCre}*Tsc1*$^{f/f}$ mice (Figure 4A), however, the total numbers of YFP^+ Treg cells were quite similar between the control and *Foxp3*^{YFPCre}*Tsc1*$^{f/f}$ mice (Figure 4B). Although analysis of the surface markers of TSC1-deficient YFP^+ Treg cells displayed no alteration in the phenotype or activation status of Treg cells (Supplemental Figure 5), we found that TSC1-deficient Treg cells exhibited a high proliferative response in vitro, as reflected in the increased expression of Ki67 (Figure 4C, upper panel). Furthermore, TSC1-deficient Treg cells were more resistant to cell death than WT Treg cells, as assessed by 7-AAD staining 72 hours after culture with anti-CD3 and anti-CD28 (Figure 4C, lower panel).

Next, we examined the in vivo suppressive function of TSC1-deficient Treg cells by adoptive transfer into *Rag1*$^{-/-}$ mice of sorted $CD4^+CD45RB^{lo}YFP^+$ ($CD45.2^+$) Treg cells together with $CD4^+CD45RB^{hi}$ ($CD45.1^+$) naive T cells. Similar to the recipient mice given Treg cells sorted from *Cd4*^{Cre}*Tsc1*$^{f/f}$ mice (Figure 3C), the mice that received TSC1-deficient YFP^+ Treg cells showed body weight loss of about 5% of their initial weight (Figure 4D) and an increased ratio of naive T cells/Treg cells (Figure 4E), without affecting the overall expansion of Treg cells (Figure 4F) in all organs analyzed. Moreover, we observed a higher frequency of IL-17–producing $CD45.1^+CD4^+$ T cells, whereas the rise in frequency of IFN-γ–producing cells was relatively moderate in the recipient mice transferred with TSC1-deficient YFP^+ Treg cells (Figure 4G). To determine whether the attenuated suppressive activity of TSC1-deficient Treg cells is associated with the loss of Foxp3 expression, we assessed Foxp3 expression by flow cytometry (Figure 4, H and I). We found a downregulation of Foxp3 expression in transferred $CD45.2^+CD4^+$ Treg cells sorted from *Foxp3*^{YFPCre}*Tsc1*$^{f/f}$ mice and observed a more substantial reduction in MLNs and cLP, suggesting a correlation between the attenuated suppressive activity and the loss of Foxp3 expression in the recipient mice given TSC1-deficient YFP^+ Treg cells. Collectively, these results indicate that TSC1 is required to fully retain the suppressive function and Foxp3 expression of Treg cells under inflammatory conditions.

TSC1 deficiency reprograms Treg cells to become Th17-like effector T cells. We then examined effector cytokine production from $CD45.2^+CD4^+$ Treg cells that were cotransferred into *Rag1*$^{-/-}$ mice with $CD45.1^+CD4^+CD45RB^{hi}$ naive T cells. IL-17 production was increased in both the YFP^- and YFP^+ populations of transferred TSC1-deficient Treg cells (Figure 5A). In order to trace the fates of $Foxp3^+$ Treg cells, we bred *Foxp3*^{YFPCre}*Tsc1*$^{l/l}$ mice expressing a YFP-Cre recombinase fusion protein from the Foxp3 promoter, with the reporter mice carrying a Cre-inducible loxP-flanked red fluorescent protein (RFP) gene in the ROSA26 locus (26) (referred to herein as *Foxp3*^{YFPCre}*R26*^{RFP}*Tsc1*$^{f/f}$). About 10% to 20% of $CD4^+RFP^+$ T cells were from a YFP-negative population that we call ex-Treg cells (Figure 5B, upper panel) and, indeed, the loss of Foxp3 expression in RFP^+YFP^- (ex-Treg) cells was confirmed by flow cytometry (Figure 5B, lower panel). We then detected TSC1 deletion in both RFP^+YFP^- (ex-Treg) and RFP^+YFP^+ Treg cells from *Foxp3*^{YFPCre}*R26*^{RFP}*Tsc1*$^{f/f}$ mice by immunoblotting and confirmed that RFP^+YFP^- T cells had escaped from RFP^+YFP^+ Treg cells (Figure 5C). There was a significant induction in the levels of cytokines such as IL-1β and IL-17 when examined by a Bio-Plex multicytokine assay in sorted TSC1-deficient $CD4^+RFP^+YFP^+$ Treg cells compared with those found in WT Treg cells (Figure 5D, right panel). Interestingly, RFP^+YFP^- (ex-Treg) T cells produced much higher amounts of overall effector cytokines than $CD4^+RFP^+YFP^+$ Treg cells, and the levels of IFN-γ and IL-17 secretion by TSC1-deficient RFP^+YFP^- (ex-Treg) Treg cells were significantly increased, suggesting that ex-Treg cells converted from TSC1-deficient Treg cells seem to acquire a phenotype similar to that of TSC1-deficient effector T cells (Figure 5D, left panel). As a negative control, we measured cytokine production in $CD4^+RFP^-YFP^-$ (naive) T cells sorted from *Foxp3*^{YFPCre}*R26*^{RFP}*Tsc*$^{+/+}$ or *Foxp3*^{YFPCre}*R26*^{RFP}*Tsc1*$^{f/f}$ mice that have intact TSC1 expression and found that cytokine production was similar between the two strains of mice (Figure 5E). We further confirmed the conversion of the population of TSC1-deficient $Foxp3^+$ Treg cells into Th17-like T cells by using an in vitro conversion assay. The secretion of IL-17 from TSC1-deficient YFP^+ Treg cells was profoundly upregulated by in vitro culture with IL-6 and TGF-β (Figure 5F). In addition, TSC1-deficient RFP^+YFP^+ Treg cells, when adoptively transferred into *Rag1*$^{-/-}$ mice, displayed a substantial loss of Foxp3 expression (Figure 5G) and an increased IL-17–producing fraction in both RFP^+YFP^+ and RFP^+YFP^-

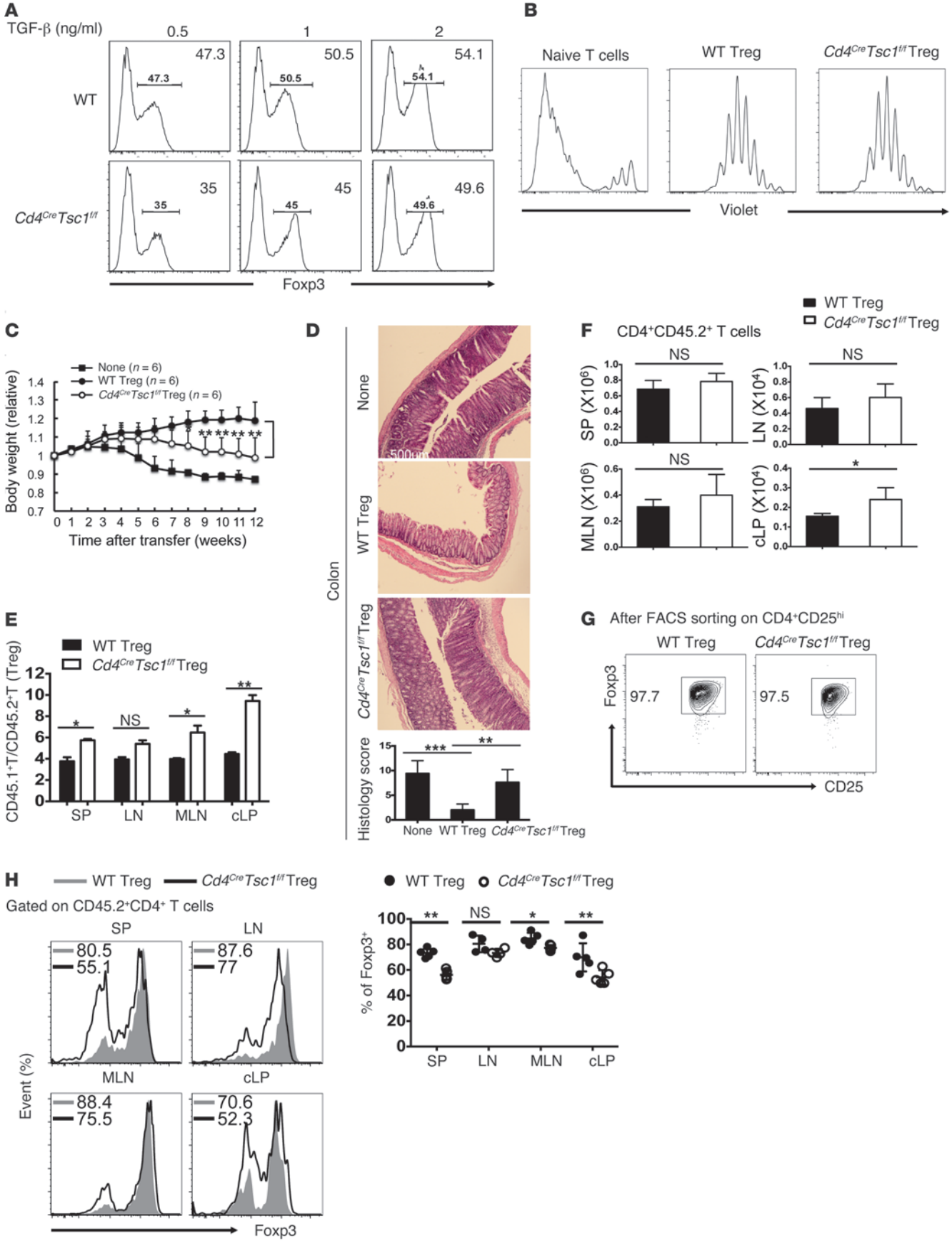
A
TGF-β (ng/ml)
0.5
1
2
WT
Cd4CreTsc1f/f
47.3
50.5
54.1
35
45
49.6
Foxp3
B
Naive T cells
WT Treg
Cd4CreTsc1f/f Treg
Violet
C
None (n = 6)
WT Treg (n = 6)
Cd4CreTsc1f/f Treg (n = 6)
Body weight (relative)
Time after transfer (weeks)
D
Colon
None
WT Treg
Cd4CreTsc1f/f Treg
500 μm
Histology score
None
WT Treg
Cd4CreTsc1f/f Treg
E
WT Treg
Cd4CreTsc1f/f Treg
CD45.1+T/CD45.2+T (Treg)
SP
LN
MLN
cLP
F
CD4+CD45.2+ T cells
WT Treg
Cd4CreTsc1f/f Treg
SP (X10^6)
LN (X10^4)
MLN (X10^6)
cLP (X10^4)
NS
G
After FACS sorting on CD4+CD25hi
WT Treg
Cd4CreTsc1f/f Treg
Foxp3
97.7
97.5
CD25
H
WT Treg
Cd4CreTsc1f/f Treg
Gated on CD45.2+CD4+ T cells
SP
LN
MLN
cLP
80.5
55.1
87.6
77
88.4
75.5
70.6
52.3
Event (%)
Foxp3
% of Foxp3+

Figure 3
Treg cells from *Cd4^{cre}Tsc1$^{f/f}$* mice have a defect in colitis suppression. (**A**) Sorted naive CD4$^+$CD62L$^+$CD25$^-$ T cells from WT and *Cd4^{Cre}Tsc1$^{f/f}$* mice were stimulated with anti-CD3/CD28 in the presence of the indicated concentrations of TGF-β. Induction of Foxp3$^+$ Treg cells was examined by flow cytometry on day 4. (**B**) Cells in **A** were cocultured with Violet-labeled CD4$^+$CD25$^-$ naive T cells at a 1:1 ratio in the presence of irradiated T cell–depleted splenocytes and anti-CD3. Violet dilution was assessed 4 days later by flow cytometry. Data are representative of three to five independent experiments (**A** and **B**). (**C**) *Rag1$^{-/-}$* mice were given sorted WT or TSC1-deficient CD4$^+$CD25$^+$ (CD45.2$^+$) Treg cells, together with CD4$^+$CD45RB^{hi} (CD45.1$^+$) T cells or CD4$^+$CD45RB^{hi} (CD45.1$^+$) T cells alone (None). Weight loss in individual mice was monitored every week for 12 weeks. (**D**–**F**) H&E staining and colon histological scores. Original magnification, ×100 (**D**); ratios of CD4$^+$CD45RB^{hi} (CD45.1$^+$) to CD4$^+$CD25$^+$ (CD45.2$^+$) Treg cells in the SP, LNs, MLNs, and cLP (**E**); absolute numbers of CD4$^+$CD45.2$^+$ T cells (**F**) in *Rag1$^{-/-}$* recipient mice, as in **C**, 12 weeks after transfer. (**G** and **H**) Flow cytometric analysis of Foxp3$^+$ expression in sorted CD4$^+$CD45RB^{lo}CD25$^+$ Treg cells before adoptive transfer (**G**) or 12 weeks after transfer (**H**) in *Rag1$^{-/-}$* recipient mice, as in **C**. Data are compiled from (**C**, **E**, and **F**) or representative of (**D** and **H**) three independent experiments with two mice each. Error bars indicate the mean ± SD. **P* < 0.05, ***P* < 0.01, and ****P* < 0.001 by two-tailed, unpaired Student's *t* test.

populations, although a profound increase in the IFN-γ–producing fraction was found only in RFP$^+$YFP$^-$ (ex-Treg) T cells (Figure 5H). Overall, these data indicate that TSC1 plays an important role in preventing Treg reprogramming into Th17-like effector T cells.

TSC1 deficiency promotes the acquisition of a Th17-like effector phenotype in Treg cells in an intrinsic manner. Since Treg cells in lymphopenic mice undergo homeostatic peripheral expansion, we examined female *Foxp3$^{YFPCre/+}$Tsc1$^{f/f}$* mice to confirm whether the conversion of Treg cells into Th17-like effector T cells occurs in an intrinsic manner due to TSC1 deficiency. These TSC1-deficient female mice heterozygous for *Foxp3^{Cre}* have both TSC1-deficient and -sufficient Treg cells that are distinguished by YFP expression. Indeed, YFP-positive or -negative cell populations coexisted in both CD4$^+$CD25$^+$ and CD4$^+$Foxp3$^+$ Treg cells (Figure 6A). Consistent with the result under lymphopenic conditions, YFP$^+$ Treg (*Tsc1$^{-/-}$*) cells sorted by CD4, CD25, and NRP1 produced significantly higher levels of IL-17 than YFP$^-$ (*Tsc1$^{+/+}$*) Treg cells when assessed by a Bio-Plex multicytokine assay (Figure 6B). The frequency of IL-17–expressing cells was also increased in CD4$^+$Foxp3$^+$YFP$^+$ Treg cells upon PMA/ionomycin stimulation in various organs analyzed (Figure 6C). Furthermore, to see the effect of TSC1 deletion on Treg cell integrity, we monitored 7-month-old *Foxp3^{YFPCre}R26^{RFP}Tsc1$^{f/f}$* mice. These older mice exhibited increases in an effector/memory phenotype (Supplemental Figure 6B) and modest increases in lymphoid aggregates and infiltration in colon (data not shown), together with an elevated population of RFP$^+$YFP$^-$ (ex-Treg) Treg cells (Supplemental Figure 6A). Collectively, these data reinforce the importance of TSC1 in retaining Treg cell identity and immune homeostasis.

S6K1 is involved in IL-17 production in TSC1-deficient T cells. To understand the molecular mechanisms by which TSC1 regulates Th17 response, we examined the downstream signaling events in TSC1-deficient T cells. Consistent with a previous study (15), phosphorylation of the mTORC1 substrate S6K1 was increased in TSC1-deficient T cells upon TCR/CD28 stimulation, whereas phosphorylation of mTORC2 downstream substrates Foxo1 and Foxo3a was reduced (Figure 7A). We found that the expression level of GRB10, which was recently identified as a target of mTORC1 (27, 28), was increased. To examine whether these mTORC1 targets are functionally involved in altered Th17 differentiation of TSC1-deficient T cells, we performed retrovirus-based knockdown of S6K1 or GRB10 expression by synthesizing small hairpin RNAs that were constructed into the murine stem cell virus–based (MSCV-based) pLMP-GFP retroviral vector. We selected the probe with the highest knockdown efficiency by validation in mouse primary T cells (data not shown) and retrovirally transduced it into mouse bone marrow cells from WT or *CD4^{cre}Tsc1$^{f/f}$* mice. Then, S6K1 shRNA– or GRB10 shRNA–expressing chimeric mice were generated by bone marrow transplantation into lethally irradiated CD45.1 congenic B6 recipient mice. Eight weeks after reconstitution, newly reconstituted CD4$^+$ T cells (CD45.2$^+$GFP$^+$) expressing either control or S6K1 or GRB10 shRNA were sorted from the spleen of bone marrow chimeric mice (Figure 7B, upper panel), and the efficient reduction of S6K1 or GRB10 expression was verified by immunoblotting in the shRNA-expressing CD4$^+$ T cells (Figure 7B, lower panel). When sorted naive CD4$^+$ T cells were cultured under polarizing conditions for Th17 differentiation, S6K1 shRNA–expressing WT T cells displayed reduced Th17 differentiation. Importantly, S6K1 knockdown in TSC1-deficient T cells markedly reduced the differentiation of naive T cells into a Th17 subset (Figure 7C). The level of IL-17 was also significantly decreased in the culture supernatants of S6K1 shRNA–expressing TSC1-deficient T cells (Figure 7D). However, the effect of GRB10 knockdown on Th17 differentiation was quite limited. We also observed hyperphosphorylation of S6K1 in TSC1-deficient YFP$^+$ Treg cells (Figure 7E) and performed further knockdown of S6K1 expression in both WT and TSC1-deficient YFP$^+$ Treg cells by using the MSCV-based pLMP-mAmetrine retroviral vector to distinguish from the expression of YFP (Figure 7F). Our examination of the cytokine profile by a Bio-Plex multicytokine assay revealed a significant reduction of IL-1β and IL-17 secretion in culture supernatants of sorted TSC1-deficient YFP$^+$mAmetrine$^+$ Treg cells (Figure 7G). These observations implicate a critical role for TSC1-mediated regulation of mTORC1/S6K1 signaling in IL-17 production in both conventional CD4$^+$ T cells and Treg cells.

Additional Foxo3a ablation promotes Treg-to-Th17-like cell conversion. To understand the role of attenuated Foxo1/Foxo3a phosphorylation in regulating Treg cell plasticity in the absence of TSC1, we generated double-knockout mice lacking TSC1 and Foxo3a and bred them with the double-reporter mice (referred to herein as *Foxp3^{YFPCre}R26^{RFP}Tsc1$^{f/f}$Foxo3a$^{f/f}$*). We found that the population of RFP$^+$YFP$^-$ (ex-Treg) T cells (Figure 8A) and the surface phenotype (data not shown) of TSC1/Foxo3a double-deficient Treg cells were similar to those observed in TSC1 single-deficient Treg cells under normal conditions. However, when stimulated with anti-CD3 and anti-CD28, TSC1/Foxo3a double deficiency induced a robust production of IL-17 in RFP$^+$YFP$^+$ Treg cells (Figure 8B, right panel), and even greater amounts of effector cytokines were secreted in TSC1/Foxo3a double-deficient RFP$^+$YFP$^-$ (ex-Treg) T cells (Figure 8B, left panel). We found that the increased IL-17 production in both TSC1- and TSC1/Foxo3a–deficient Treg cells was reduced by the treatment of mTOR inhibitor rapamycin (Figure 8C). These

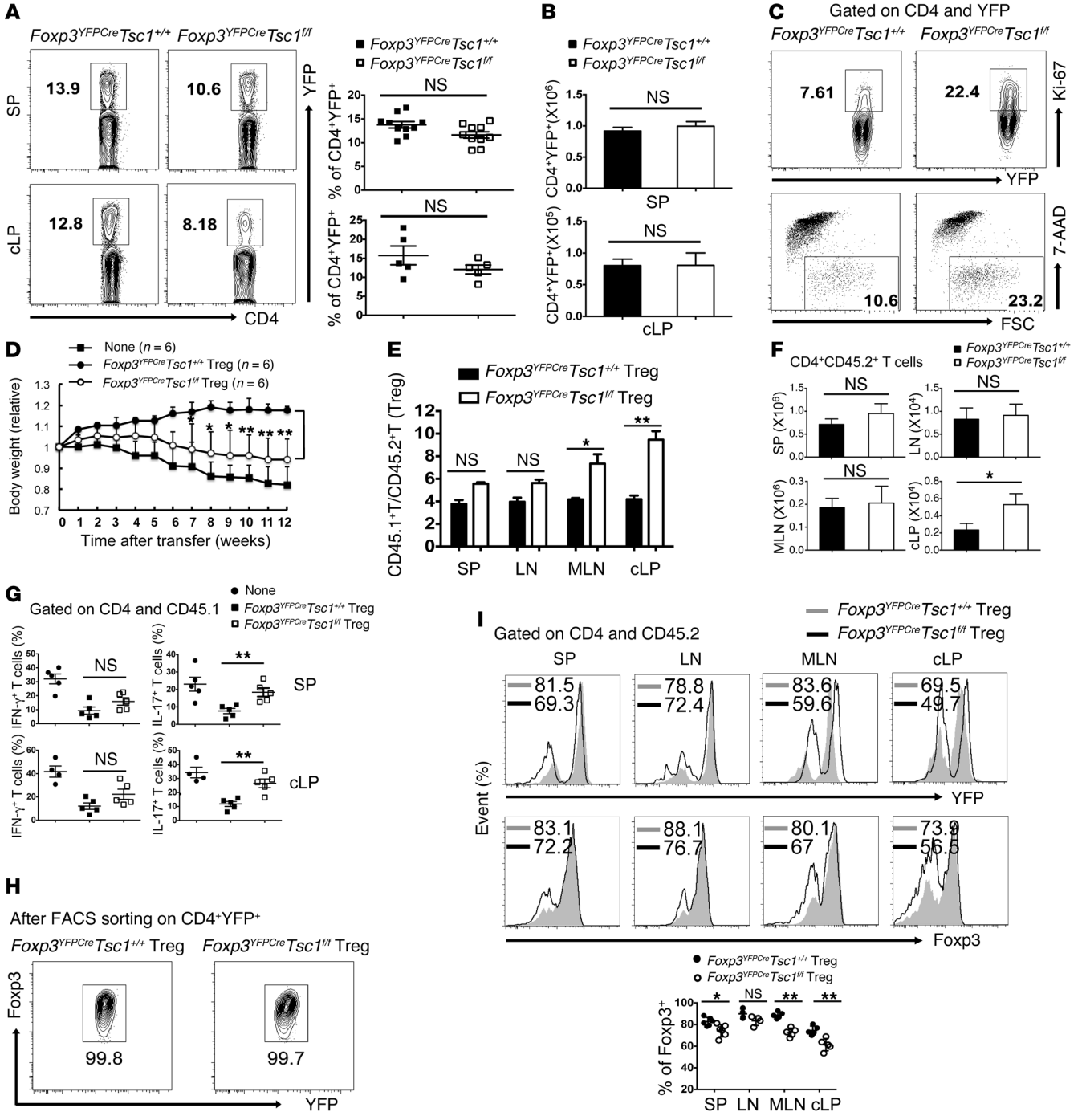

Figure 4

TSC1 deficiency in Foxp3+ Treg cells results in loss of Treg function under inflammatory condition. (**A** and **B**) Flow cytometric analysis (left), frequencies (right) of YFP expression (**A**), and absolute numbers of CD4+YFP+ T cells (**B**) from spleen or cLP of *Foxp3*^{YFPCre}*Tsc1*$^{+/+}$ and *Foxp3*^{YFPCre}*Tsc1*$^{f/f}$ mice. (**C**) Flow cytometric analysis of Ki-67 expression in CD4+YFP+T cells (upper panel) and 7-AAD staining in CD4+YFP+T cells 48 hours after anti-CD3/CD28 stimulation (lower panel) in *Foxp3*^{YFPCre}*Tsc1*$^{+/+}$ and *Foxp3*^{YFPCre}*Tsc1*$^{f/f}$ mice. Data are representative of (**A** and **C**) or compiled from (**B**) three independent experiments. Error bars indicate the mean ± SD by two-tailed, unpaired Student's *t* test. (**D**) *Rag1*$^{-/-}$ mice were given sorted CD4+YFP+ (CD45.2+) Treg cells from *Foxp3*^{YFPCre}*Tsc1*$^{+/+}$ or *Foxp3*^{YFPCre}*Tsc1*$^{f/f}$ mice, together with CD4+CD45RB^{hi} (CD45.1+) T cells, or CD4+CD45RB^{hi} (CD45.1+) T cells alone (None). Weight loss of individual mice was monitored every week for 12 weeks. (**E**–**G**) Ratios of CD4+CD45RB^{high} (CD45.1+) to CD4+YFP+ (CD45.2+) Treg cells in the SP, LNs, MLNs, and cLP (**E**); absolute numbers of CD4+CD45.2+ T (Treg) cells (**F**); frequencies of the indicated cytokine-producing CD4+CD45.1+ T cells in spleen and cLP (**G**) in *Rag1*$^{-/-}$ recipient mice as in **D** 12 weeks after transfer. (**H** and **I**) Flow cytometric analysis of Foxp3+ expression in sorted CD4+CD45RB^{lo}YFP+ Treg cells before adoptive transfer (**H**) or 12 weeks after transfer (**I**) in *Rag1*$^{-/-}$ recipient mice as in **D**. Data are compiled from (**D**–**G**) or representative of (**I**) three independent experiments with two mice each. Error bars indicate the mean ± SD. *$P < 0.05$ and **$P < 0.01$ by two-tailed, unpaired Student's *t* test.

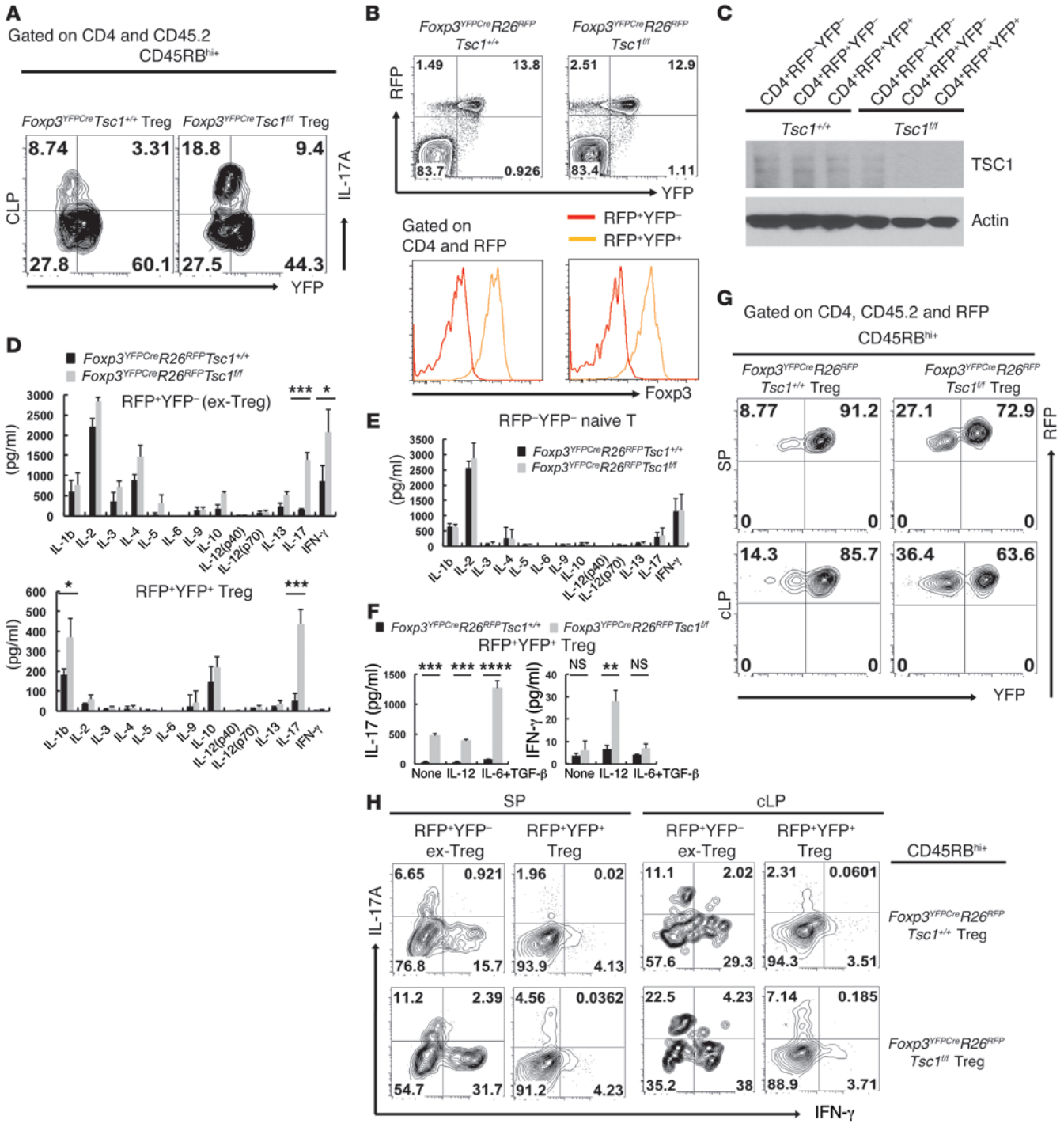

Figure 5

TSC1-deficient Foxp3⁺ Treg cells produce IL-17 and convert into effector-like T cells. (**A**) Flow cytometric analysis of IL-17A–producing CD45.2⁺CD4⁺ Treg cells from cLP of recipient mice as in Figure 4D, 6 weeks after transfer, followed by restimulation with PMA/ionomycin for 6 hours. (**B**) Flow cytometric analysis of YFP and RFP expression in CD4⁺ T cells (upper panel) or Foxp3 expression in CD4⁺RFP⁺ T cells (lower panel) in *Foxp3*^{YFPCre}*R26*^{RFP}*Tsc1*$^{+/+}$ and *Foxp3*^{YFPCre}*R26*^{RFP}*Tsc1*$^{f/f}$ mice. (**C**) Immunoblot analysis of TSC1 in sorted CD4⁺RFP⁻YFP⁻, CD4⁺RFP⁺YFP⁻, and CD4⁺RFP⁺YFP⁺ T cells from *Foxp3*^{YFPCre}*R26*^{RFP}*Tsc1*$^{+/+}$ and *Foxp3*^{YFPCre}*R26*^{RFP}*Tsc1*$^{f/f}$ mice. (**D** and **E**) Sorted CD4⁺RFP⁺YFP⁺ Treg cells (**D**, right panel) or CD4⁺RFP⁺YFP⁻ ex-Treg cells (**D**, left panel), or CD4⁺CD62L⁺RFP⁻YFP⁻ naive T cells (**E**) from *Foxp3*^{YFPCre}*R26*^{RFP}*Tsc1*$^{+/+}$ and *Foxp3*^{YFPCre}*R26*^{RFP}*Tsc1*$^{f/f}$ mice were stimulated with anti-CD3/CD28 for 36 hours. Cytokine production was measured by Bio-Plex multicytokine assay. (**F**) Sorted CD4⁺RFP⁺YFP⁺ Treg cells were stimulated with anti-CD3/CD28, IL-2, and the indicated cytokines for 48 hours. Cytokine production was measured by Bio-Plex multicytokine assay. (**G** and **H**) *Rag1*$^{-/-}$ mice were given sorted CD4⁺RFP⁺YFP⁺ (CD45.2⁺) Treg cells from *Foxp3*^{YFPCre}*R26*^{RFP}*Tsc1*$^{+/+}$ or *Foxp3*^{YFPCre}*R26*^{RFP}*Tsc1*$^{f/f}$ mice, together with CD4⁺CD45RB^{hi} (CD45.1⁺) T cells. Flow cytometric analysis of RFP and YFP expression (**G**) or cytokine production (**H**) in CD45.2⁺CD4⁺RFP⁺ T cells of the recipient mice 6 weeks after transfer. Data are representative of (**A**, **B**, **G**, and **H**) or compiled from (**D**–**F**) two to five independent experiments. Error bars indicate the mean ± SD. **P* < 0.05, ***P* < 0.01, ****P* < 0.001, and *****P* < 0.0001 by two-tailed, unpaired Student's *t* test.

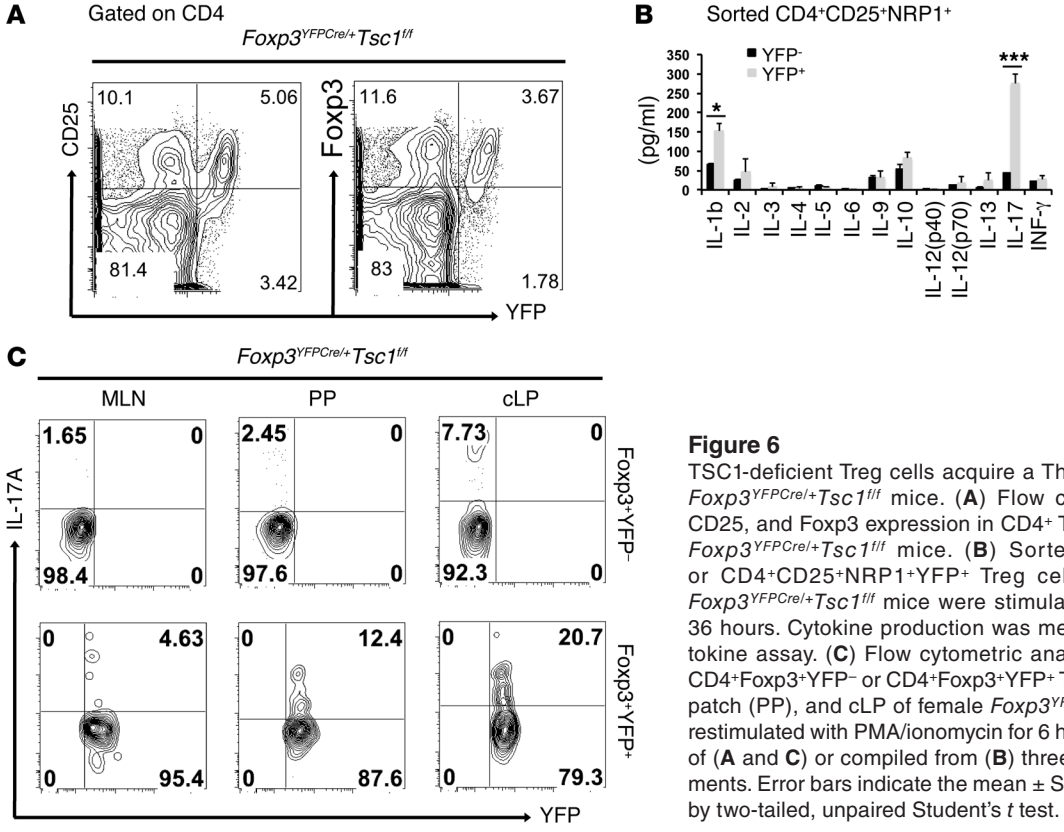

Figure 6
TSC1-deficient Treg cells acquire a Th17-like phenotype in female *Foxp3*$^{YFPCre/+}$*Tsc1*$^{f/f}$ mice. (**A**) Flow cytometric analysis of YFP, CD25, and Foxp3 expression in CD4$^+$ T cells from spleen of female *Foxp3*$^{YFPCre/+}$*Tsc1*$^{f/f}$ mice. (**B**) Sorted CD4$^+$CD25$^+$NRP1$^+$YFP$^-$ or CD4$^+$CD25$^+$NRP1$^+$YFP$^+$ Treg cells from spleen of female *Foxp3*$^{YFPCre/+}$*Tsc1*$^{f/f}$ mice were stimulated with anti-CD3/CD28 for 36 hours. Cytokine production was measured by Bio-Plex multicytokine assay. (**C**) Flow cytometric analysis of IL-17 production by CD4$^+$Foxp3$^+$YFP$^-$ or CD4$^+$Foxp3$^+$YFP$^+$ Treg cells from MLNs, Peyer's patch (PP), and cLP of female *Foxp3*$^{YFPCre/+}$*Tsc1*$^{f/f}$ mice. Cells were restimulated with PMA/ionomycin for 6 hours. Data are representative of (**A** and **C**) or compiled from (**B**) three to four independent experiments. Error bars indicate the mean ± SD. *$P < 0.05$ and ***$P < 0.001$ by two-tailed, unpaired Student's *t* test.

results indicate that reversing the effects of mTORC2 inactivation by Foxo3a deletion in TSC1-deficient Treg cells facilitates the reprogramming of Treg cells to become Th17-like effector T cells, which further demonstrates the role of TSC1 as a critical regulator between effector T cells and Treg cells via the differential modulation of mTORC1 and mTORC2 activity.

Discussion

In the present study, we demonstrate that TSC1 plays a critical role in maintaining stable Foxp3 expression and the suppressive function of Treg cells by preventing their conversion into Th17-like effector T cells in response to environmental stimuli. We found that aged *Cd4*^{Cre}*Tsc1*$^{f/f}$ mice developed spontaneous multiorgan inflammation as a consequence of hyperactivation of T cells by greater activity of mTORC1. TSC1 deficiency in CD4$^+$ T cells resulted in elevated Th1 and Th17 responses. Although the development of CD4$^+$CD25$^+$Foxp3$^+$ natural Treg (nTreg) cells and TGF-β–induced Treg cells is quite similar in WT and *Cd4*^{Cre}*Tsc1*$^{f/f}$ mice under normal conditions, robust Th1 and Th17 cell responses are accompanied by a reduced accumulation of Foxp3$^+$ Treg cells in *Cd4*^{Cre}*Tsc1*$^{f/f}$ mice during chronic intestinal inflammation. Furthermore, cotransfer of TSC1-deficient CD4$^+$CD25$^+$ Treg cells with WT naive T cells into lymphopenic mice failed to suppress colitis development, which demonstrates that TSC1 is required to instruct both effector T and Treg cells to respond appropriately to environmental cues.

The importance of TSC1 as an intrinsic regulator in maintaining Treg cell stability and function was revealed by the study of *Foxp3*^{YFPCre}*Tsc1*$^{f/f}$ mice. Interestingly, TSC1-deficient Treg cells displayed a high proliferative and survival ability at least in vitro, which is opposite to the effect of TSC1 deletion in naive T cells that has been known to affect the survival and quiescence of naive T cells (14, 15). Since regulation of the degree of metabolic demands and mTOR activity has been known to be a critical process for T cell fate determination (29), this finding suggests that the distinct difference in the requirements for mTOR activity in the respective T cell subsets is important not only in directing T cell fate, but also in maintaining their homeostasis and modulating their immunological functions.

One interesting finding of the present study is that TSC1-deficient Foxp3$^+$ Treg cells showed impaired suppressive activity and reduced Foxp3 expression only under inflammatory conditions. Furthermore, TSC1 deficiency selectively induced the conversion of Treg cells into Th17-like effector T cells. Several recent studies have shown that Treg cells lose Foxp3 expression and become "ex-Tregs" that acquire an effector memory phenotype and produce proinflammatory cytokines (19–22). However, the issue of Treg cell lineage commitment remains controversial (23, 24). In our fate-mapping study involving *Foxp3*$^{YFPCre'}$*Rosa26*^{RFP} mice, TSC1-deficient RFP$^+$YFP$^+$ Treg cells, which are considered to stably express Foxp3, produced greater amounts of IL-17 in vitro as well as in vivo after their transfer into *Rag1*$^{-/-}$ mice. More interestingly, TSC1-deficient YFP$^-$RFP$^+$ ex-Treg cells produced much higher levels of cytokines, including IL-17 and IFN-γ, compared with those found in WT ex-Treg cells. Combined with the results of the in vitro studies, our adoptive transfer study using sorted RFP$^+$YFP$^+$ Treg cells clearly demonstrates that ex-Treg (RFP$^+$YFP$^-$) fractions originate from Foxp3$^+$ Treg cells and are reprogrammed to acquire an effector memory phenotype. It is nonetheless possible that even though these cells must have expressed Foxp3 at

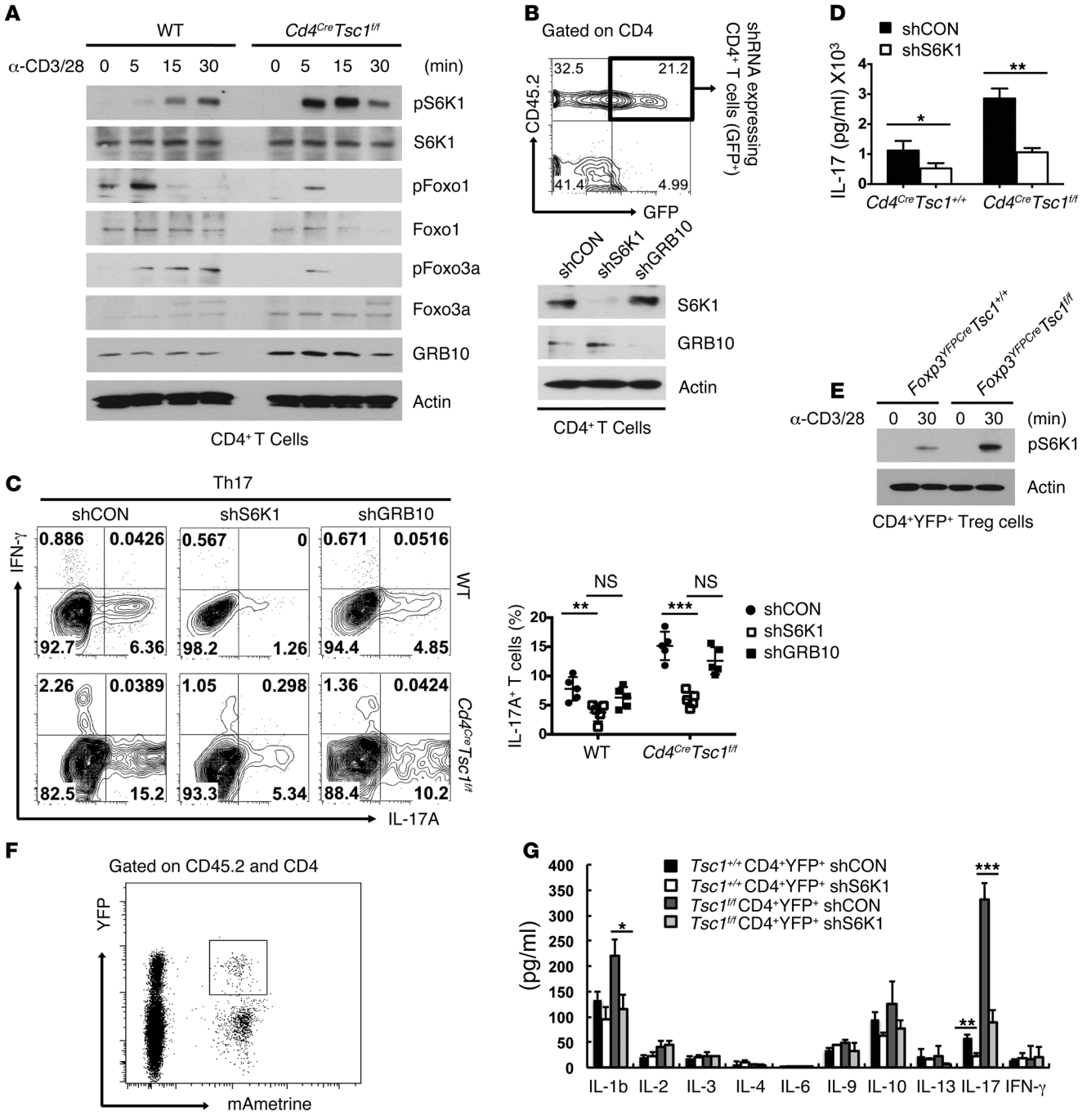

Figure 7

S6K1 knockdown in TSC1-deficient T cells leads to attenuated IL-17 production. (**A**) Analysis of the phosphorylation status of the indicated downstream targets of TSC1. CD4+ T cells from WT or *CD4^{cre}Tsc1$^{f/f}$* mice were stimulated with anti-CD3/CD28 for the indicated time periods, and the cell lysates were subjected to immunoblotting with the indicated antibodies. (**B**) Analysis of GFP expression in peripheral blood from bone marrow chimeric mice 2 months after reconstitution of control (shCON) or S6K1 or GRB10 shRNAs expressing WT or *Cd4^{Cre}Tsc1$^{f/f}$* bone marrow cells (upper panel). Immunoblot analysis of S6K1 and GRB10 was performed in sorted CD4+GFP+ T cells (lower panel). (**C** and **D**) Flow cytometric analysis (**C**, left panel), frequencies (**C**, right panel), or cytokine production (**D**) of Th17-polarized naive CD4+GFP+ T cells from bone marrow chimeric mice as in **B**. (**E**) Analysis of the phosphorylation status of S6K1 in CD4+YFP+ Treg cells. (**F**) Analysis of mAmetrine expression in peripheral blood from bone marrow chimeric mice 2 months after reconstitution of control or S6K1 shRNAs expressing *Foxp3^{YFPCre}Tsc1$^{+/+}$* or *Foxp3^{YFPCre}Tsc1$^{f/f}$* bone marrow cells. (**G**) Cytokine production in CD4+YFP+mAmetrine+ T cells from bone marrow chimeric mice as in **F** was measured by Bio-Plex multicytokine assay 36 hours after stimulation with anti-CD3/CD28. Data are representative of (**B**, **C**, and **F**) or compiled from (**D** and **G**) three to five independent experiments. Error bars indicate the mean ± SD. *P < 0.05, **P < 0.01, and ***P < 0.001 by two-tailed, unpaired Student's t test.

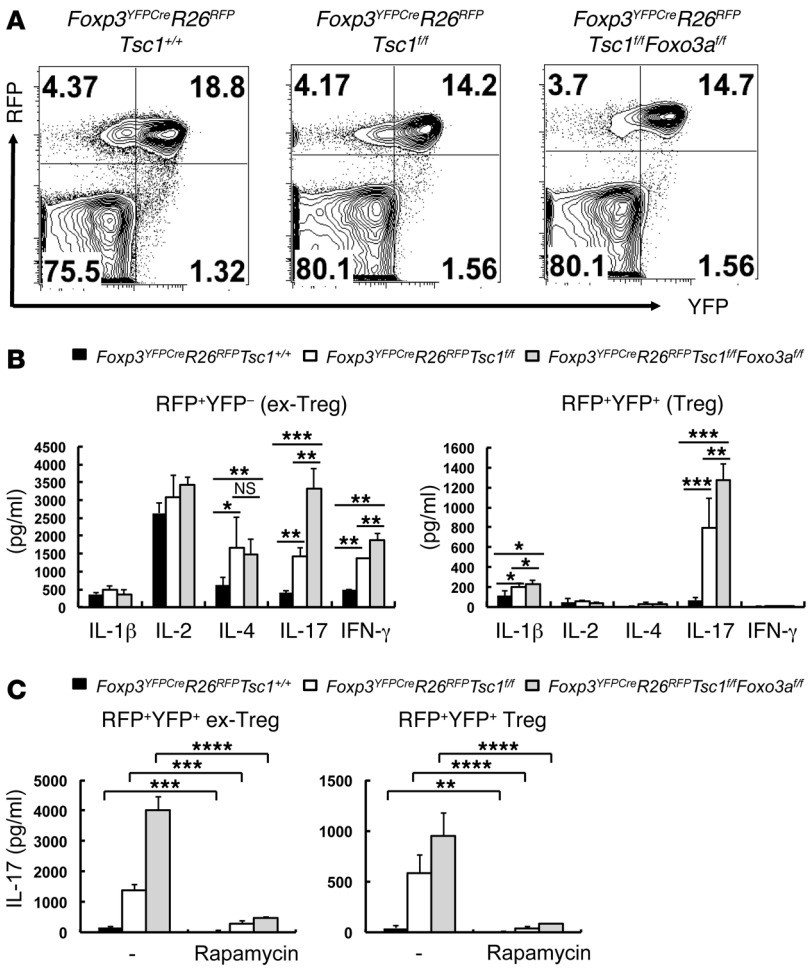

Figure 8

Double deletion of TSC1 and Foxo3a heightens Treg conversion to Th17-like cells. (**A**) Flow cytometric analysis of YFP and RFP expression in CD4+T cells of *Foxp3*^{YFPCre}*R26*^{RFP}*Tsc1*$^{+/+}$, *Foxp3*^{YFPCre}*R26*^{RFP}*Tsc1*$^{f/f}$, and *Foxp3*^{YFPCre}*R26*^{RFP}*Tsc1*$^{f/f}$*Foxo3a*$^{f/f}$ mice. (**B**) Sorted CD4+RFP+YFP+ Treg cells (right) or CD4+RFP+YFP− ex-Treg cells (left) from the mice in **A** were stimulated with anti-CD3/CD28 for 36 hours. Cytokine production was measured by Bio-Plex multicytokine assay. (**C**) Sorted CD4+RFP+YFP+ Treg cells (right) or CD4+RFP+YFP− ex-Treg cells (left) from the mice in **A** were stimulated with anti-CD3/CD28 for 72 hours in the presence or absence of 250 nM rapamycin. Cytokine production was measured by Bio-Plex multicytokine assay. Data are representative of (**A**) or compiled from (**B** and **C**) three independent experiments. Error bars indicate the mean ± SD. $^{*}P < 0.05$, $^{**}P < 0.01$, $^{***}P < 0.001$, and $^{****}P < 0.0001$ by two-tailed, unpaired Student's *t* test.

some point, this could have been due to an incomplete differentiation and commitment to become Treg cells, as opposed to a loss of Foxp3 expression by committed Treg cells. An increased acquisition of a Th17-like phenotype by TSC1-deficient Treg cells was also found in a competitive environment, although this conversion was greatly promoted under inflammatory conditions, which was probably provoked by the production of inflammatory cytokines such as IL-1 and IL-6. Furthermore, we found that aged *Foxp3*^{YFPCre}*R26*^{RFP}*Tcs1*$^{f/f}$ mice exhibited dysregulated immune homeostasis along with an increase in ex-Treg (RFP+YFP−) fractions, which provides convincing evidence that ex-Treg generation is caused by TSC1 deficiency–induced reprogramming of Treg cells under physiological conditions and not simply by aberrant homeostatic expansion in lymphopenic hosts.

Previous studies have shown the importance of mTOR signaling in the regulation of Th cell differentiation (5–7). In our study, the enhanced Th17 responses were likely associated with mTORC1-dependent signal transduction to its downstream substrate S6K1, since in vivo knockdown of S6K1 rescued the hyperresponsiveness of both IL-17–producing effector T cells and Treg cells to a remarkable extent. Although the detailed mechanism of how S6K1 is involved in the regulation of T cell lineage–specific gene expression has been poorly understood, a recent study showed a key role for S6K1 and S6K2 in Th17 differentiation via the regulation of GFI1 expression, a negative regulator of Th17 cells, and the nuclear translocation of RORγt, respectively (30). Further study of the regulatory mechanisms of S6K1 action and the role of other mTORC1 substrates, such as 4E-BP1 and GRB10 in Treg cells, is required to gain more insight into the link between TSC1/mTORC1 signaling and Th17/Treg balance.

Several recent studies have shown that mTORC2-mediated phosphorylation of downstream Foxo1 and Foxo3a inhibits Foxp3 expression (31–33). However, mTORC2 inhibition by genetic deletion of Rictor is not sufficient for Treg cell generation when mTORC1 activity remains intact (6). Since we found that heightened mTORC1 activity in TSC1-deficient T cells downregulated mTORC2 activity by negative feedback, as assessed by reduced Foxo1/3a phosphorylation, we reasoned that this reduced mTORC2 activity may compromise the effect of augmented mTORC1 activity on Treg stability and function. Indeed, Foxo3a deletion in TSC1-deficient Treg cells largely accelerated the conversion of Treg cells into Th17-like effector T cells. And furthermore, rapamycin treatment blocked this reprogramming of TSC1/Foxo3a–deficient Treg cells, even though rapamycin has been known to enhance mTORC2 activity by inhibiting mTORC1 activity, which suggests that TSC1 has a dominant role in retaining the stability and functional ability of Treg cells by maintaining an appropriate balance between mTORC1 and mTORC2 activity.

In conclusion, our studies demonstrate that TSC1 acts as a key mediator in integrating the environmental cues and immunolog-

ical signals that instruct apt responses in T cells. Under homeostatic conditions, TSC1 deficiency did not induce a significant imbalance between effector and regulatory immune responses by inhibiting mTORC2 activity. However, under inflammatory conditions, an altered cytokine environment caused impairment of TSC1-mediated mTORC1/2 regulation, which led to the dysfunction of immunological tolerance. Therefore, further studies to define the mechanism by which TSC1-mediated regulation of mTORC1/2 is linked to balancing the need to restrain inflammatory responses and simultaneously maintain the ability to mount effector responses will provide new insight for the development of therapeutic drugs to treat human immune disease.

Methods

Mice. C57BL/6, B6.SJL (CD45.1 congenic), and *Rag1*$^{-/-}$ mice were obtained from The Jackson Laboratory. Floxed TSC1 mice on a C57BL/6 background were provided by K-.L. Guan (UCSD, San Diego, California, USA). Floxed Foxo3a mice were obtained from R.A. DePinho (MD Anderson Cancer Center, Houston, Texas, USA). Foxp3-YFP-Cre mice were provided by A. Rudensky (Memorial Sloan Kettering Cancer Center, New York, New York, USA). The fate-tracing ROSA26-loxP-Stop-loxP RFP reporter mice were from H.J. Fehling (Institute of Immunology, University Clinics, Ulm, Germany). TSC1 mice were bred with CD4-Cre mice (*Cd4*^{Cre}*Tsc1*$^{f/f}$) or Foxp3-YFP-Cre mice (*Foxp3*^{YFPCre}*Tsc1*$^{f/f}$). Some of the *Foxp3*^{YFPCre}*Tsc1*$^{f/f}$ mice were further bred with the RFP reporter mice to generate *Foxp3*^{YFPCre}*R26*^{RFP}*Tsc1*$^{f/f}$ mice. For the generation of TCR transgenic mice, $OVA_{323-329}$-specific TCR transgenic OT-II mice were crossed with *Cd4*^{Cre}*Tsc1*$^{f/f}$ mice. All mice were housed in specific pathogen-free conditions.

Th cell differentiation in vitro. Sorted naive CD4$^+$CD62L$^+$CD25$^-$ T cells from WT or *Cd4*^{Cre}*Tsc1*$^{f/f}$ mice were stimulated with plate-bound anti-CD3 (3 μg/ml; 2C11; BioLegend) and soluble anti-CD28 (1 μg/ml; 37.5; Bio-Xcell) in the presence of irradiated splenocytes. Cells were cultured in Th-neutral conditions by culturing with rhIL-2 (100 U/ml), or they were polarized to Th1 cells by culturing with rhIL-2 (100 U/ml), mouse IL-12 (10 ng/ml; Peprotech), and anti-mouse IL-4 antibody (10 μg/ml; BD Biosciences). Alternatively, cells were polarized to Th17 cells by culturing with mouse IL-6 (10 ng/ml; Peprotech), human TGF-β (2 ng/ml; Peprotech), anti-mouse IFN-γ antibody (10 μg/ml; BioLegend), and anti-mouse IL-4 (10 μg/ml; BioLegend). Four days later, Th17 cells were cultured with anti-mouse IFN-γ antibody (10 μg/ml) and anti-mouse IL-4 (10 μg/ml) for an additional 2 days.

Adoptive transfer and OVA immunization. CD4$^+$ T cells from WT or *Cd4*^{Cre}*Tsc1*$^{f/f}$ OT-II mice were isolated, and 1×10^6 cells were injected retro-orbitally into WT B6 CD45.1 congenic mice. The next day, the recipient mice were immunized by s.c. injection with OVA (50 μg; Grade V; Sigma-Aldrich) emulsified in CFA (Difco; BD Diagnostics). Six days after immunization, cells were collected from the spleen and inguinal lymph nodes and cultured with $OVA_{323-339}$ peptide (10 μg/ml; AnaSpec) for 8 hours at 37°C in the presence of Golgi stop (BD Biosciences). The intracellular cytokine profiles were analyzed by flow cytometry.

Multicytokine assay. To measure the production of multiple cytokines, sorted CD4$^+$RFP$^+$YFP$^+$, CD4$^+$RFP$^+$YFP$^-$, or CD4$^+$RFP$^-$YFP$^-$ T cells were stimulated with plate-bound anti-CD3 (3 μg/ml) and soluble anti-CD28 (1 μg/ml) for 36 hours. Then, the culture supernatants were collected, and cytokines were detected using the Multi-Plex cytokine kit from Bio-Rad according to the manufacturer's instructions.

KLH immunization. WT or *Cd4*^{Cre}*Tsc1*$^{f/f}$ OT-II mice were immunized by s.c. injection with keyhole limpet hemocyanin (KLH, 50 μg; Sigma-Aldrich) emulsified in CFA. Six days after immunization, CD4$^+$ T cells were collected from the spleen and cultured with KLH for 72 hours at 37°C. Supernatants were collected, and cytokines were detected using a Multi-Plex cytokine kit from Bio-Rad according to the manufacturer's instructions.

Colitis induction. Mice were given 2% (wt/vol) DSS dissolved in the drinking water for 7 days and sacrificed between 2 and 4 weeks after stopping DSS. Body weights were recorded every other day during the DSS treatment and removal periods. Histological assessment of colitis was performed by H&E staining and analyzed by microscopy. For the T cell transfer model of colitis, sorted naive CD4$^+$CD25$^-$CD45RB^{hi} T cells (4×10^5 cells/mouse) from WT CD45.1 congenic mice were coinjected i.v. into C57BL/6 *Rag1*$^{-/-}$ mice with sorted CD4$^+$CD25$^+$CD45RB^{lo} Treg cells (1×10^5 cells/mouse) from WT or *Cd4*^{Cre}*Tsc1*$^{f/f}$ C57BL/6 mice, or with CD4$^+$YFP$^+$ Treg cells from *Foxp3*^{YFPCre}*Tsc1*$^{+/+}$ or *Foxp3*^{YFPCre}*Tsc1*$^{f/f}$ C57BL/6 mice. Recipient *Rag1*$^{-/-}$ mice were monitored weekly for 12 weeks.

Isolation of cells from cLP. The cecal patch was excised from the colons and then the colons were opened longitudinally, washed of fecal contents, cut into 1-cm-long pieces, and incubated three times for 20 minutes each in HBSS with 5% FBS and 2 mM EDTA at 37°C, with agitation to remove epithelial cells. After incubation, the remaining tissue was minced and further incubated for 20 minutes in HBSS with 5% FBS and 3 mg/ml type IV collagenase (Sigma-Aldrich) at 37°C with agitation. Cell suspensions were collected and passed through a 70-μm strainer and pelleted by centrifugation at 300 *g*.

In vitro Treg cell generation and suppression assay. Sorted naive CD4$^+$CD62L$^+$CD25$^-$ T cells (2×10^5) from WT or *Cd4*^{Cre}*Tsc1*$^{f/f}$ mice were stimulated with plate-bound anti-CD3 (2 μg/ml) and soluble anti-CD28 (1 μg/ml), together with the indicated concentrations of rhTGF-β (PeproTech) in 96-well flat-bottom plates for 3 days. For the in vitro suppression assay, sorted naive CD4$^+$CD62L$^+$CD25$^-$ T cells (5×10^4 cells) were labeled with 5 μM CellTrace Violet (Invitrogen) for 10 minutes at 37°C in PBS and 0.1% BSA and were then cocultured with in vitro iTregs (5×10^4 cells) from WT or *Cd4*^{Cre}*Tsc1*$^{f/f}$ mice in the presence of T cell–depleted splenocytes (1×10^5 cells) and soluble anti-CD3. Four days later cells were harvested, and Violet dilution was measured by flow cytometric analysis.

Immunoblotting. Antibodies against TSC1, S6K1, phospho-S6K1 (pS6K1), Foxo1, phospho-Foxo1 (pFoxo1), Foxo3a, and phospho-Foxo3a (pFoxo3a) were purchased from Cell Signaling Technology. Anti-GRB10 was purchased from Proteintech, and anti-actin was purchased from Millipore. Cells were lysed with NP-40 lysis buffer (1% NP-40, 20 mM Tris-HCl, pH 7.5, 150 mM NaCl, 5 mM EDTA, 50 mM NaF, 2 mM Na_3VO_4, and 10 μg/ml each of aprotinin and leupeptin) or were lysed with 1X SDS sample buffer (50 mM Tris-HCl, pH 6.8, 100 mM DTT, 2% SDS, and 10% glycerol). Proteins were separated by SDS-PAGE and transferred to nitrocellulose membranes (Bio-Rad). Membranes were visualized by Western blotting with an enhanced chemiluminescence detection system (GE Healthcare). When necessary, the membranes were stripped by incubation in stripping buffer (Thermo Fisher Scientific) for 15 minutes with constant agitation, washed, and then reprobed with various other antibodies.

Retroviral transduction and bone marrow reconstitution. To construct S6K1 shRNA vector, oligonucleotides were cloned into an LMP vector according to the manufacturer's protocol (Open Biosystems). Oligonucleotide sequences were the following: S6K1 shRNA, 5′-TGCTGTTGACAGTGAGCGATGGCTCCATCTGTACTTGAAATAGTGAAGCCACAGATGT-3′; and GRB10 shRNA, 5′-TGCTGTTGACAGTGAGCGCGCCTTCAGACTGCTCAAGTACTAGTGAAGCCACAGATGT-3′. To generate bone marrow chimeric mice expressing S6K1 or GRB10 shRNA, Plat-E cells were transfected with 3 μg of LMP vector with 9 μl of TransIT-LT1 (Mirus). At 48 hours, the culture supernatant containing retrovirus was collected. Mature T cell–depleted bone marrow cells from WT or *Cd4*^{Cre}*Tsc1*$^{f/f}$ mice were cultured for 24 hours in IL-3 (10 ng/ml), IL-6 (10 ng/ml), and SCF (100 ng/ml) (all from Peptrotech) containing complete DMEM before initial retroviral infection, and they were infected with retrovirus together with 5 μg/ml polybrene by centrifuging cells at 800 *g* for 60 minutes at room temperature. Two days

after infection, retrovirally transduced bone marrow cells were injected into lethally irradiated (9 Gy) C57BL/6 recipient mice. Recipient mice were sacrificed and analyzed 8 weeks after reconstitution.

Statistics. Statistical analyses were performed using a two-tailed, unpaired Student's *t* test. A *P* value less than 0.05 was considered statistically significant.

Study approval. All animal experimental protocols were approved by the IACUC of the La Jolla Institute for Allergy and Immunology.

Acknowledgments

We thank K-.L. Guan, R.A. DePinho, A. Rudendsky, and H.J. Fehling for sharing their valuable mice. J.H. Lee provided technical help. Y. Park is supported in part by a fellowship from the National Research Foundation of Korea (NRF-2011-357-E00030). This work was supported by an NIH-NIAID program project grant (PO1AI089624).

Received for publication March 8, 2013, and accepted in revised form September 12, 2013.

Address correspondence to: Yun-Cai Liu, Division of Cell Biology, La Jolla Institute for Allergy and Immunology, 9420 Athena Circle, La Jolla, California 92037, USA. Phone: 858.752.6810; Fax: 858.752.6986; E-mail: yuncail@liai.org.

1. Guertin DA, Sabatini DM. Defining the role of mTOR in cancer. *Cancer Cell*. 2007;12(1):9–22.
2. Hay N, Sonenberg N. Upstream and downstream of mTOR. *Genes Dev*. 2004;18(16):1926–1945.
3. Yang Q, Guan KL. Expanding mTOR signaling. *Cell Res*. 2007;17(8):666–681.
4. Araki K, et al. mTOR regulates memory CD8 T-cell differentiation. *Nature*. 2009;460(7251):108–112.
5. Delgoffe GM, et al. The mTOR kinase differentially regulates effector and regulatory T cell lineage commitment. *Immunity*. 2009;30(6):832–844.
6. Delgoffe GM, et al. The kinase mTOR regulates the differentiation of helper T cells through the selective activation of signaling by mTORC1 and mTORC2. *Nat Immunol*. 2011;12(4):295–303.
7. Lee K, et al. Mammalian target of rapamycin protein complex 2 regulates differentiation of Th1 and Th2 cell subsets via distinct signaling pathways. *Immunity*. 2010;32(6):743–753.
8. Peter C, Waldmann H, Cobbold SP. mTOR signalling and metabolic regulation of T cell differentiation. *Curr Opin Immunol*. 2010;22(5):655–661.
9. Delgoffe GM, Kole TP, Cotter RJ, Powell JD. Enhanced interaction between Hsp90 and raptor regulates mTOR signaling upon T cell activation. *Mol Immunol*. 2009;46(13):2694–2698.
10. Procaccini C, et al. An oscillatory switch in mTOR kinase activity sets regulatory T cell responsiveness. *Immunity*. 2010;33(6):929–941.
11. Yurchenko E, et al. Inflammation-driven reprogramming of CD4+ Foxp3+ regulatory T cells into pathogenic Th1/Th17 T effectors is abrogated by mTOR inhibition in vivo. *PLoS One*. 2012; 7(4):e35572.
12. Huang J, Manning BD. The TSC1-TSC2 complex: a molecular switchboard controlling cell growth. *Biochem J*. 2008;412(2):179–190.
13. O'Brien TF, et al. Regulation of T-cell survival and mitochondrial homeostasis by TSC1. *Eur J Immunol*. 2011;41(11):3361–3370.
14. Wu Q, et al. The tuberous sclerosis complex-mammalian target of rapamycin pathway maintains the quiescence and survival of naive T cells. *J Immunol*. 2011;187(3):1106–1112.
15. Yang K, Neale G, Green DR, He W, Chi H. The tumor suppressor Tsc1 enforces quiescence of naive T cells to promote immune homeostasis and function. *Nat Immunol*. 2011;12(9):888–897.
16. Zhang L, et al. TSC1/2 signaling complex is essential for peripheral naive CD8+ T cell survival and homeostasis in mice. *PLoS One*. 2012;7(2):e30592.
17. Xie DL, Wu J, Lou YL, Zhong XP. Tumor suppressor TSC1 is critical for T-cell anergy. *Proc Natl Acad Sci U S A*. 2012;109(35):14152–14157.
18. Koch MA, Tucker-Heard G, Perdue NR, Killebrew JR, Urdahl KB, Campbell DJ. The transcription factor T-bet controls regulatory T cell homeostasis and function during type 1 inflammation. *Nat Immunol*. 2009;10(6):595–602.
19. Komatsu N, Mariotti-Ferrandiz ME, Wang Y, Malissen B, Waldmann H, Hori S. Heterogeneity of natural Foxp3+ T cells: a committed regulatory T-cell lineage and an uncommitted minor population retaining plasticity. *Proc Natl Acad Sci U S A*. 2009; 106(6):1903–1908.
20. Murai M, et al. Interleukin 10 acts on regulatory T cells to maintain expression of the transcription factor Foxp3 and suppressive function in mice with colitis. *Nat Immunol*. 2009;10(11):1178–1184.
21. Takahashi R, et al. SOCS1 is essential for regulatory T cell functions by preventing loss of Foxp3 expression as well as IFN-{gamma} and IL-17A production. *J Exp Med*. 2011;208(10):2055–2067.
22. Zhou X, et al. Instability of the transcription factor Foxp3 leads to the generation of pathogenic memory T cells in vivo. *Nat Immunol*. 2009; 10(9):1000–1007.
23. Rubtsov YP, et al. Stability of the regulatory T cell lineage in vivo. *Science*. 2010;329(5999):1667–1671.
24. Miyao T, et al. Plasticity of Foxp3(+) T cells reflects promiscuous Foxp3 expression in conventional T cells but not reprogramming of regulatory T cells. *Immunity*. 2012;36(2):262–275.
25. Maynard CL, Weaver CT. Intestinal effector T cells in health and disease. *Immunity*. 2009;31(3):389–400.
26. Luche H, Weber O, Nageswara Rao T, Blum C, Fehling HJ. Faithful activation of an extra-bright red fluorescent protein in "knock-in" Cre-reporter mice ideally suited for lineage tracing studies. *Eur J Immunol*. 2007;37:43–53.
27. Hsu PP, et al. The mTOR-regulated phosphoproteome reveals a mechanism of mTORC1-mediated inhibition of growth factor signaling. *Science*. 2011; 332(6035):1317–1322.
28. Yu Y, et al. Phosphoproteomic analysis identifies Grb10 as an mTORC1 substrate that negatively regulates insulin signaling. *Science*. 2011; 332(6035):1322–1326.
29. Powell JD, Delgoffe GM. The mammalian target of rapamycin: linking T cell differentiation, function, and metabolism. *Immunity*. 2010;33(3):301–311.
30. Kurebayashi Y, et al. PI3K-Akt-mTORC1-S6K1/2 axis controls Th17 differentiation by regulating Gfi1 expression and nuclear translocation of RORγ. *Cell Rep*. 2012;1(4):360–373.
31. Harada Y, Elly C, Ying G, Paik JH, DePinho RA, Liu YC. Transcription factors Foxo3a and Foxo1 couple the E3 ligase Cbl-b to the induction of Foxp3 expression in induced regulatory T cells. *J Exp Med*. 2010;207(7):1381–1391.
32. Kerdiles YM, et al. Foxo transcription factors control regulatory T cell development and function. *Immunity*. 2010;33(6):890–904.
33. Ouyang W, Beckett O, Ma Q, Paik JH, DePinho RA, Li MO. Foxo proteins cooperatively control the differentiation of Foxp3+ regulatory T cells. *Nat Immunol*. 2010;11(7):618–627.